ELSEVIER

Atmospheric Research 35 (1995) 127–138

ATMOSPHERIC RESEARCH

Ice microphysics and climatic temperature feedback

Szu-cheng Ou and Kuo-Nan Liou

Department of Meteorology/CARSS, University of Utah, Salt Lake City, UT 84112, USA

Received 18 December, 1992; revised version accepted 16 July, 1993

Abstract

The potential effects of ice microphysics involving ice crystal size distribution and ice water path (IWP) on climatic temperature perturbations are investigated by using a one-dimensional radiative-turbulent climate model. We define a mean effective size, denoting the width of ice crystals weighted by the geometric cross section area, to represent ice crystal size distribution. Based on aircraft measurements, both the mean effective size and IWP are related to temperature and may be parameterized as functions of temperature. The radiative properties of cirrus clouds are further parameterized in terms of these two basic cloud physics parameters. Using CO_2 doubling as the radiative forcing, feedbacks among temperature, the mean effective size and IWP, and the radiative properties of clouds are analyzed from the model results. We show that overall, a positive feedback associated with ice microphysics and the coupled radiative transfer is produced by temperature increase.

1. Introduction

The importance of clouds in climate and climatic perturbations has been recognized based on a number of observational and modeling studies. Radiation budgets at the top of the atmosphere and at the surface are both significantly modulated by the presence of clouds in the atmosphere. Middle and low clouds are primarily responsible for the reflection of sunlight. Hence, their presence would cool the surface below. However, typical cirrus clouds (temperature lower than $-20°$) are relatively opaque to thermal IR radiation but transparent to solar radiation. Their presence would tend to warm the underlying surface. The competition between the solar albedo and IR greenhouse effects involving cirrus clouds is dependent on such factors as the cloud position, microphysics and their radiative properties. At this point, the role of cirrus clouds in climate remains one of

SSDI 0169-8095(94)00014-5

the the least understood components of the weather and climate systems (Liou, 1986).

Numerical experiments using one-dimensional radiative-convective models, in which the transfer of solar and IR radiative fluxes can be treated more comprehensively, have been carried out to understand the potential role of clouds in climate. Charlock (1982) and Somerville and Remer (1984) showed that the cloud liquid water content (*LWC*) increases as a result of greenhouse warming, leading to a negative feedback. Using an interactive cloud and climate model, Liou et al. (1985) and Ou and Liou (1987) also found that overall, clouds exert a negative feedback in response to temperature increases produced by positive radiative forcings. More recently, Liou and Ou (1989) incorporated microphysical parameterizations in terms of cloud particle sizes in a cloud and climate model and demonstrated that in addition to the cloud cover and cloud *LWC*, cloud particle size can also be an important factor in climate feedback analysis. Somerville and Iacobellis (1987) investigated feedbacks of the cirrus cloud optical thickness to surface warming due to increasing concentration of greenhouse gases and showed that a positive feedback is produced from the one-dimensional radiative-convective model. Stephens et al. (1990) illustrated that feedbacks of the cirrus radiative properties to surface temperatures can be either positive or negative, depending on cloud microphysics and the mean single-scattering properties of cloud particles.

In this paper, we investigate the potential effects of cirrus radiative feedbacks through the *IWP* and ice crystal size distribution on climate perturbations. Section 2 presents the parameterizations of the ice microphysical and radiative properties of cirrus clouds. Results from the one-dimensional model simulation are discussed in Section 3. Finally, conclusions are given in Section 4.

2. Parameterizations of the microphysical and radiative properties of cirrus clouds

2.1. Mean effective size

From aircraft measurements, it has been determined that cirrus clouds are largely composed of columns, plates and bullet rosettes (Heymsfield, 1975; Heymsfield et al., 1990). Based on laboratory and field experiments, the length, L, and the width, D, of an ice crystal may be related by a power form: $D=aL^b$, where a and b are empirical coefficients (Auer and Veal, 1970; Heymsfield, 1972; Hobbs et al., 1975). Thus, the ice crystal size distribution, $n(L)$, can be defined in terms of the length or the maximum dimension of ice crystals.

Ice crystals will scatter an amount of light in proportion to their cross-section areas. Thus, for the purpose of radiative transfer parameterization, it is physically appropriate to define a mean effective size (D_e) to represent the mean properties of ice crystal size distribution in the form

$$D_e = \int_{L_{min}}^{L_{max}} D^2 Ln(L) \mathrm{d}L \Big/ \int_{L_{min}}^{L_{max}} DLn(L) \mathrm{d}L. \quad (1)$$

In view of the fact that D is related to L, the definition of the mean effective size is equivalent to the ratio of the third to second moments of ice crystal size distribution.

We may relate D_e to the cloud temperature through appropriate microphysics observations. Based on a large number of cirrus microphysical data collected by optical probes during flights over midlatitudes, Heymsfield and Platt (1984) determined that ice crystal size distribution can be represented by a general power form in terms of length and ice water content (IWC) as follows:

$$n(L) = AL^B \cdot IWC, \quad (2)$$

where IWC is in units of g/m^3, and A and B are empirical coefficients determined from the measured data. The values of A,B and IWC depend on temperature. It follows that $n(L)$ is also a function of temperature. Thus, given a temperature, $n(L)$ can be determined. Subsequently, D_e can be obtained from Eq. (1). The lower limit L_{min} is set at 20 μm, based on the limitations of optical probes. The upper limit L_{max} is prescribed using the observed maximum crystal length. Fig. 1 shows D_e values derived from the coefficients given by Heymsfield and Platt (1984) for eight temperature intervals. To relate D_e to cloud temperature, T_c(°C), directly, the following parameterized polynomial relationship has been derived using a statistical procedure:

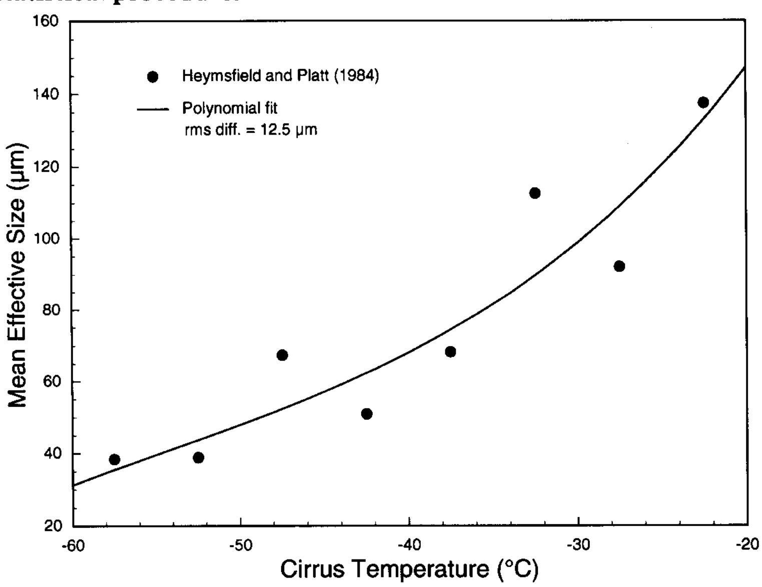

Fig. 1. Values of ice crystal mean effective size obtained from Eqs. (1) and (2) for eight temperature intervals. These values are obtained based on the data presented by Heymsfield and Platt (1984). The curve represents the best-fit polynomial parameterization.

$$D_e = \sum_{n=0}^{3} c_n T_c^n, \quad (3)$$

where $c_0 = 326.3$, $c_1 = 12.42$, $c_2 = 0.197$ and $c_3 = 0.0012$. The root-mean-square difference between the D_e values computed from Eq. (1) and from the polynomial fitting is about 12.5 μm. From Eq. (3), it is evident that D_e increases with increasing T_c. Recent microphysics measurements from aircraft reported by Heymsfield et al. (1990) also indicate that D_e tends to increase with increasing temperature.

2.2. Ice water path

IWP is the product of *IWC* and cloud thickness Δz. Both *IWC* and Δz may be related to temperature based on observations. Fig. 2 shows the average *IWC* as a function of temperature in the range from -20 to -60°C derived from the dataset collected by Heymsfield and Platt (1984). The standard deviation in each temperature interval is denoted by vertical bars. The steepest increase of the average *IWC* occurs from -42 to -37°C. Liou (1986) presented a parameterization of *IWC* as a function of temperature based on this dataset in the form

$$[\ln(IWC) + 7.6]/4 = \exp[2.443 \times 10^{-4} (|T_c| - 20)^{2.455}], \; T_c < -20°C. \quad (4)$$

The differences between the parameterized values (the solid curve) and the sam-

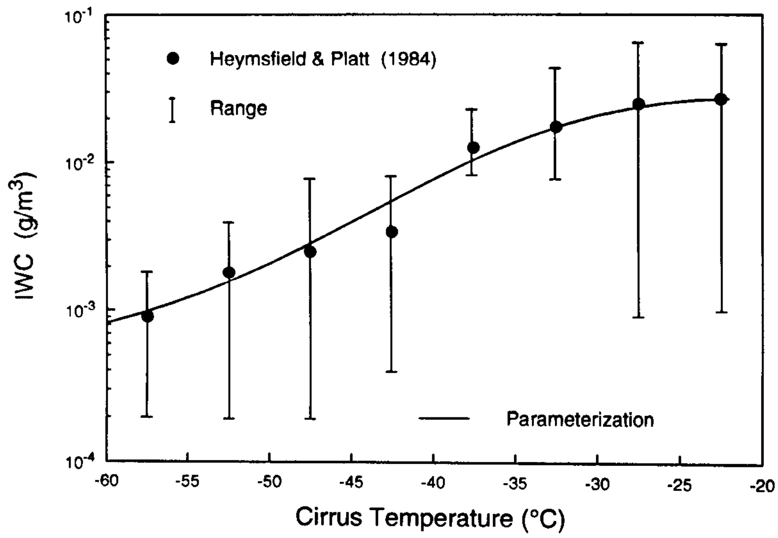

Fig. 2. Values of the average *IWC* derived from the dataset of Heymsfield and Platt (1984) as a function of temperature. The curve represents the best-fit polynomial parameterization.

ple mean values denoted by black dots are much smaller than the standard deviations of the measured data.

Based on lidar observations collected at Aspendale and Darwin in Australia, Platt et al. (1987) determined the average mid-cloud altitudes. They showed that mid-latitude cirrus clouds occur most frequently between −20 to −60°C, in agreement with the result obtained by Heymsfield and Platt (1984). The highest frequency of cirrus occurrence is at −45°C, which corresponds roughly to an altitude of 9 km. For the present climatic sensitivity studies, cirrus clouds are placed between −40 to −50°C in the one-dimensional radiative-convective model.

Platt et al. (1987) also presented the mean cirrus cloud thickness versus the mid-cloud temperature. In midlatitude areas, the mean cirrus cloud thicknesses range from 1 to 3.5 km with standard deviations between 1 and 2 km. The mean cirrus cloud thickness increases with temperature from −70 to −35°C. However, it decreases with increasing temperature from −35 to −10°C. The mean cirrus cloud thickness, which is a function of temperature, varies less in the summer than in the winter. Also, cirrus clouds occurring in the summer are thinner than those in the winter. Based on the observed data for cloud thicknesses in the midlatitude region, Platt and Harshvardhan (1988) developed the following two-part parameterizations:

$$\Delta z = \begin{cases} 0.0456 T_c + 4.7 & (-70°\mathrm{C} < T_c < -35°\mathrm{C}) \\ -0.065 T_c + 0.725 & (-35°\mathrm{C} < T_c < -10°\mathrm{C}), \end{cases} \quad (5)$$

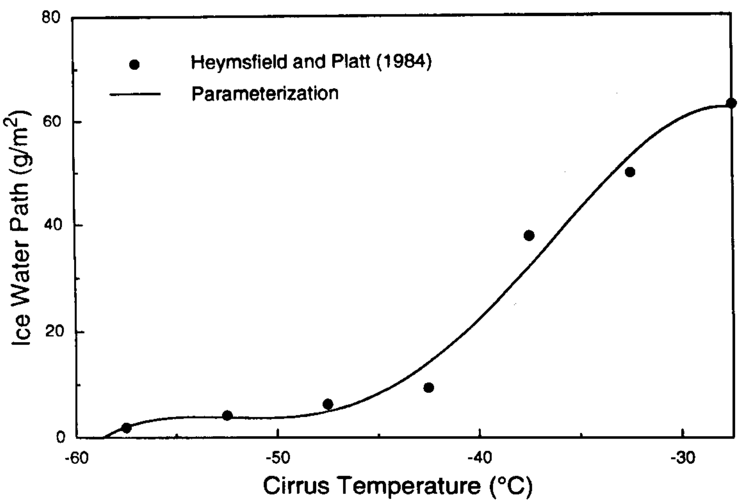

Fig. 3. Values of the average *IWP* derived from the datasets of Heymsfield and Platt (1984) and Platt et al. (1987) as a function of temperature. The curve represents the best-fit polynomial parameterization.

where Δz is in km. The parameterized values are computed from the averages of the summer and winter mean cirrus cloud thicknesses.

Based on the parameterizations of the mean cirrus cloud thickness and the mean *IWC*, the mean *IWP* can be directly expressed in terms of temperature. To effectively incorporate the temperature dependence of *IWP* in the climate model, we have developed the following parameterization equation based on a statistical procedure:

$$IWP = \sum_{n=0}^{4} d_n T_c^n, \quad -60°C < T_c < -20°C. \tag{6}$$

Both the measured values and parameterization results are shown in Fig. 3 We note that between −45 and −35°C a significant increase of *IWP* occurs (from 9.39 to 37.7 g/m^2). This increase is produced by the combined effect of the maximum thickness and the sharp increase in *IWC* at about −40°C.

2.3. Radiative properties

The IR and solar radiative properties of cirrus clouds are parameterized in terms of *IWP* and D_e. We divide the IR and solar spectra into 12 and 6 bands, respectively. The radiative transfer methodology used is the delta-four-stream approximation developed by Liou et al. (1988). This approximation can achieve a relative accuracy within 5% under all atmospheric conditions. Gaseous absorption in the scattering atmosphere is effectively accounted for by using the correlated *k*-distribution method (Fu and Liou, 1992). The scattering and absorption properties of hexagonal ice crystals whose size parameters are larger than about 30 are determined from the geometrical ray-tracing technique developed by Takano and Liou (1989). For size parameters that are less than 30, the Mie-type solution for spheroids developed by Asano and Sato (1980) is used.

Single-scattering computations are carried out for a number of ice crystal size distributions reported by Heymsfield and Platt (1984) and recently derived from the FIRE cirrus experiments. Based on physical reasoning, the single-scattering albedo, the extinction coefficient, and the expansion coefficients in Legendre polynomials for the phase function are parameterized using the third-order polynomial in terms of the mean effective size. The accuracy of the overall parameterization is within about 5%. Fig. 4a and b shows solar albedo and IR emissivity as functions of *IWP* and D_e. A cosine of the solar zenith angle of 0.5 is used in the solar radiative transfer calculations. For a given D_e, solar albedo increases with increasing *IWP*. However, for a given *IWP*, a cloud with a smaller D_e reflects more solar radiation because of larger optical depth. The IR emissivity is significantly dependent on both D_e and *IWP*. Fig. 4b also depicts the emissivity parameterization presented by Liou and Wittman (1979), which corresponds to the emissivity curve for $D_e = 50$ μm derived from the present study. Similar to solar albedo, IR emissivity increases with *IWP*, but decreases if D_e increases.

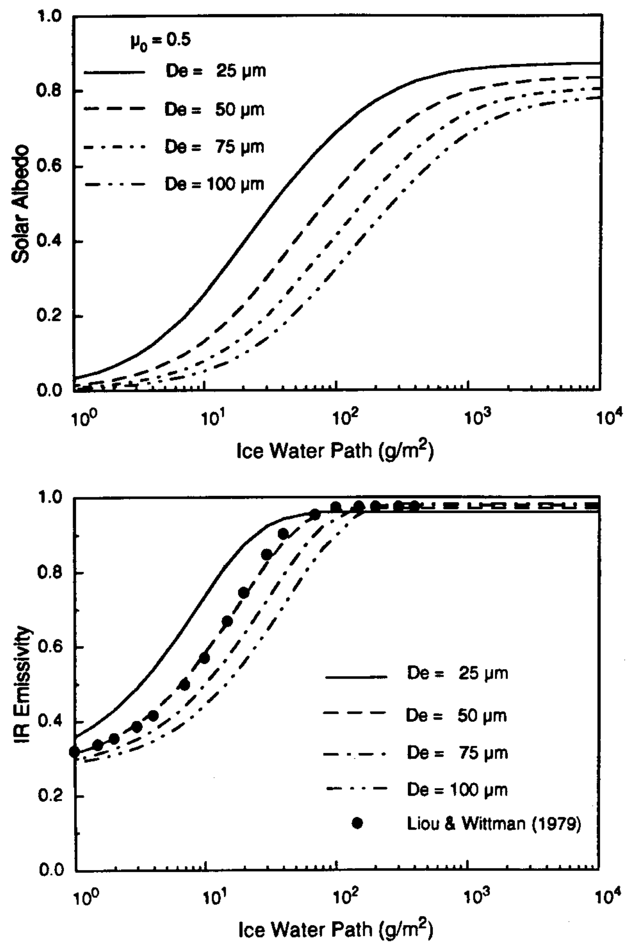

Fig. 4. The solar albedo (a) and IR emissivity (b) of cirrus clouds as functions of *IWP* and D_e.

3. Climatic effects of ice crystal size distribution and ice water path

The preceding parameterization for ice microphysics, in terms of temperature-dependent mean effective size and ice water path, and for the radiative properties of cirrus clouds defined by these two parameters, is incorporated in the one-dimensional cloud and climate model developed by Liou and Ou (1989). We first run the model under a $1\times CO_2$ (330 ppm) condition, which is referred to as the control run. Under this run the surface temperature deviates from the climatological mean (288.1 K) by no more than 0.1 K. It should be noted that the present one-dimensional model does not generate different types of clouds that occur in realistic atmospheres. However, the cloud fractional cover and *LWC* are computed in each model layer, from which the position, cover and *LWC* for high, middle and low clouds are derived based on statistical averaging procedures (Liou et al., 1985). This allows us to compare the model cloud covers with the cloud climatology presented by London (1957). From London's data, we find that the cloud covers for high, middle and low cloud types are 0.156, 0.188 and 0.350, respectively, with a total cloud cover of 0.511. The present model generates a total cloud cover of 0.516. The cloud cover for each cloud type differs from London's results by no more than 0.03. The cloud *LWC*'s for middle and low clouds are 0.083 and 0.099 g/m^3, respectively. These values are within the range of available observational statistics (Matveev, 1984; Isaac, 1991).

The radiative properties of cirrus clouds were computed based on the parameterizations described in Section 2. The IR emissivity, reflectivity and transmissivity for cirrus clouds in the control run are 0.706, 0.126 and 0.282, respectively. Based on the present parameterizations, the emissivity is determined by the *IWP*, which is in turn controlled by temperature. At a temperature of $-42.5\,^\circ$C, at which cirrus clouds are assumed to form, $IWP = 17\ g/m^2$. The solar transmittance and albedo for cirrus clouds at $\mu_0 = 0.5$ are 0.82 and 0.17, respectively. As noted previously the *IWP*'s in the model are determined from the temperature via the parameterization Eq. (6), which is derived from aircraft measurement of *IWC*'s and lidar observations of cloud thicknesses associated with midlatitude cirrus cloud systems. Observations of thin cirrus have been extremely limited. Thus, the issue of the representation of thin cirrus on global climate would require further research efforts.

A series of numerical experiments has been performed to simulate the climatic perturbations due to the doubling of CO_2 concentration. Four possible feedbacks produced by ice microphysics are considered. These are denoted as $\epsilon(D_e)$, $\epsilon(IWP)$, $\alpha(D_e)$ and $\alpha(IWP)$, where ϵ and α are IR emissivity and solar albedo, respectively, and $y(x)$ implies feedback of y due to changes in x. The prime objective of this study is to investigate climatic feedbacks involving ice microphysics and radiative transfer. For this reason, the *LWC* and cloud cover for low and middle clouds and the cloud cover for cirrus clouds are prescribed in all the simulation studies. In the first simulation, we fix the radiative properties of cirrus clouds that correspond to the condition of no feedback. The resulting surface temperature change, ΔT_s, is 2.41 K, as shown in Fig. 5. This value is within the ΔT_s range of 2–4 K, determined from general circulation model simulations (Schlesinger and Mitchell, 1987). Feedbacks to temperature in the model are modulated by the radiative properties of clouds, principally the cloud IR emissivity, ϵ, and the cloud solar albedo, α, which are functions of the temperature-dependent D_e and *IWP*, as shown in Fig. 4. Let ϵ_o and α_o represent the IR emissivity and solar albedo corresponding to the present climate condition. The perturbed values may then be written in the forms:

$$\epsilon = \epsilon_o + \frac{d\epsilon}{dT}\Delta T = \epsilon_o + \left(\frac{\partial \epsilon}{\partial IWP}\frac{dIWP}{dT} + \frac{\partial \epsilon}{\partial D_e}\frac{dD_e}{dT} \right)\Delta T,$$

$$\alpha = \alpha_o + \frac{d\alpha}{dT}\Delta T = \alpha_o + \left(\frac{\partial \alpha}{\partial IWP}\frac{dIWP}{dT} + \frac{\partial \alpha}{\partial D_e}\frac{dD_e}{dT} \right)\Delta T. \tag{7}$$

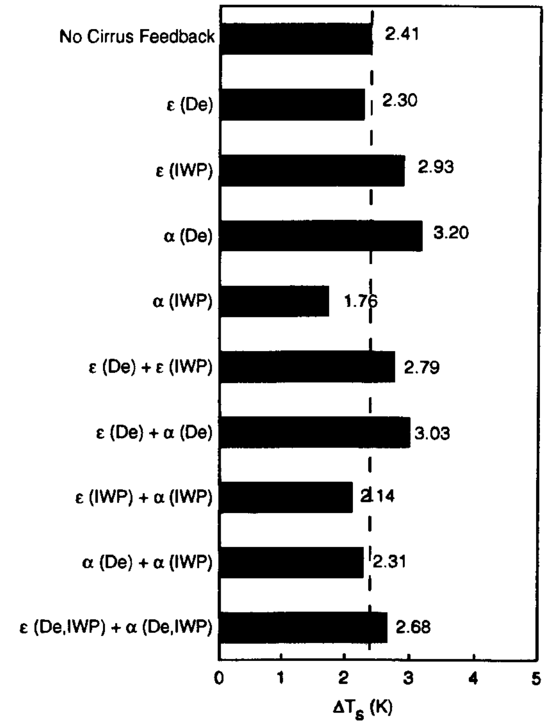

Fig. 5. Surface temperature perturbations ΔT_s due to doubling of CO_2 involving various components of cirrus radiative feedbacks. (See text for further explanation).

The terms in the parentheses represent feedbacks due to radiation (ϵ,α) and ice microphysics (IWP, D_e).

On the basis of the ice microphysics analysis presented in Section 2, when temperature increases, both IWP and D_e increase, implying that the cloud contains more mass and that the mean ice crystal size becomes larger. Furthermore, in accord with the results presented in Fig. 5, $\partial\epsilon/\partial IWP$ and $\partial\alpha/\partial IWP$ are both positive. However, $\partial\epsilon/\partial D_e$ and $\partial\alpha/\partial D_e$ are both negative. The IR greenhouse effect is largely controlled by IR emissivity, which increases as the IWP increases, implying a positive feedback. The positive feedback is also evident when solar albedo decreases, as a result of a larger mean ice crystal size. However, negative feedbacks are related to the reduction of IR emissivity and the increase of solar albedo via the increase of mean ice crystal size and IWP, respectively. Quantitative temperature changes associated with these individual feedbacks are displayed in Fig. 5.

From the preceding analysis it is clear that there are competing effects between the increases in D_e and IWP associated with IR emissivity and solar albedo. Four additional runs were carried out that included variations in IR emissivity due to both D_e and IWP (case 1); variations in solar albedo due to both D_e and IWP

(case 2); variations in both IR emissivity and solar albedo due solely to D_e (case 3); and variations in both IR emissivity and solar albedo due solely to *IWP* (case 4). The temperature change results are also depicted in Fig. 5. In case 1, the effect of *IWP* is greater than that of D_e, resulting in a positive temperature increase. In case 2, the effect of D_e is slightly smaller, resulting in a small temperature decrease. In case 3, the increase in D_e leads to the reduction of solar albedo, which outweighs the reduction in IR emissivity. As a result, a positive temperature increase is produced. In case 4, the increase in solar albedo due to increasing *IWP* outweighs the increase in IR emissivity, leading to a negative temperature feedback. In view of these perturbation results, it is evident that both *IWP* and D_e must be included in the feedback analysis. The past investigations on the cloud and climate feedbacks have only been concerned with *IWP* without consideration of mean effective size. For this reason, negative feedbacks (case 4) have frequently been reported. Finally, combining all four feedbacks simultaneously in the model, a net positive feedback is produced, resulting in a surface temperature increase of about 0.27 K.

4. Conclusions

We have carried out feedback analyses using a one-dimensional cloud and climate model involving ice microphysics and coupled radiative transfer. Parameterizations of the mean effective size, D_e, representing ice crystal size distribution, and *IWP*, the product of *IWC* and cloud thickness Δz, have been carried out by using the available measured data. Large uncertainties exist in the observed data. Both D_e and *IWP* are dependent upon temperature. The radiative properties of cirrus clouds are parameterized in terms of both D_e and *IWP* based on a scheme that has been recently developed.

The IR cloud emissivity, ϵ, and the solar cloud albedo, α, have been analyzed with respect to D_e and *IWP*. Increasing ϵ would lead to an increase of the IR greenhouse effect, while increasing α would result in an increase of the solar albedo effect. These processes represent two competing effects. Moreover, temperature increase would lead to increases in both *IWP* and D_e. An increase in *IWP* would produce larger cloud emissivity and cloud albedo. However, an increase in D_e would lead to smaller cloud emissivity and cloud albedo. Again, the increases in D_e and *IWP* represent two competing effects. We have performed model simulations to assess the quantitative effects of individual and combined events on the temperature feedbacks. Consideration of the *IWP* feedback only would produce a negative feedback, a result that has been reported by a number of previous researchers. However, the effect of changing D_e when temperature perturbs would lead to a significant positive feedback, primarily through the dominating solar albedo effect. Overall, we show that temperature increase due to a positive radiative forcing, such as CO_2 doubling, would lead to a positive feedback produced by the increase of mean ice crystal size.

Acknowledgements

Research contained in this paper has been supported by the NASA grant NAG5-1050, the National Science Foundation grant ATM-90-24217 and the Air Force Office of Scientific Research grant AFOSR-91-0039.

References

Asano, S. and Sato, M., 1980. Light scattering by randomly oriented spheroidal particles. Appl. Opt., 19: 962–974.
Auer, A.H., Jr. and Veal, D.L., 1970. The dimension of ice crystals in natural clouds. J. Atmos. Sci., 27: 919–926.
Charlock, T.P., 1982. Cloud optical feedback and climate stability in a radiative-convective model. Tellus, 34: 245–254.
Fu, Q. and Liou, K.N., 1992. On the correlated k-distribution method for radiative transfer in nonhomogeneous atmospheres. J. Atmos. Sci., 49: 2139–2156.
Heymsfield, A.J., 1972. Ice crystal terminal velocities. J. Atmos. Sci., 29: 1348–1357.
Heymsfield, A., 1975. Cirrus uncinus generating cells and the evolution of cirriform clouds. Part I: Aircraft observations of the growth of the ice phase. J. Atmos. Sci., 32: 799–808.
Heymsfield, A.J. and Platt, C.M.R., 1984. A parameterization of the particle size spectrum of ice clouds in terms of the ambient temperature and the ice water content. J. Atmos. Sci., 41: 846–855.
Heymsfield, A.J., Miller, K.M. and Spinhirne, J.D., 1990. The 27–28 October 1986 FIRE IFO cirrus east study: cloud microstructure. Mon. Weather Rev., 118: 2313–2328.
Hobbs, P.V., Radke, L.F. and Atkinson, D.G., 1975. Airborne Measurements and Observations in Cirrus Clouds. AFCRL-TR-75-0249, Air Force Geophysics Laboratory, Hanscom AFB, 117 pp.
Isaac, G.A., 1991. Microphysical characteristics of Canadian Atlantic storms. Atmos. Res., 26: 339–360.
Liou, K.N., 1986. Influence of cirrus clouds on weather and climate processes: a global perspective. Mon. Weather Rev., 114: 1167–1199.
Liou, K.N. and Ou, S.C., 1989. The role of cloud microphysical processes in climate: an assessment from a one-dimensional perspective. J. Geophys. Res., 94: 8599–8607.
Liou, K.N. and Wittman, G.D., 1979. Parameterization of the radiative properties of clouds. J. Atmos. Sci., 36: 1261–1273.
Liou, K.N., Ou, S.C.S. and Lu, P.J., 1985. Interactive cloud formation and climatic temperature perturbations. J. Atmos. Sci., 42: 1969–1981.
Liou, K.N., Fu, Q. and Ackerman, T.P., 1988. A simple formulation of the delta-four-stream approximation for radiative transfer parameterizations. J. Atmos. Sci., 45: 1940–1947.
London, J., 1957. A Study of the Atmospheric Heat Balance. Final Rep., Contract AF 19(122)-166. New York Univ., 99 pp.
Matveev, L.T., 1984. Cloud Dynamics. Reidel, Dordrecht, 340 pp.
Ou, S.C. and Liou, K.N., 1987. Effects of interactive cloud cover and liquid water content programs on climatic temperature perturbations. In: K.N. Liou and X. Zhou (Editors), Atmospheric Radiation, Progress and Prospects. Science Press, Beijing, pp. 433–440.
Platt, C.M.R. and Harshvardhan, 1988. Temperature dependence of cirrus extinction: Implications for climate feedback. J. Geophys. Res., 93: 11,051–11,058.
Platt, C.M.R., Scott, J.C. and Dilley, A.C., 1987. Remote sounding of high clouds, VI, Optical properties of midlatitude and tropical cirrus. J. Atmos. Sci., 44: 729–747.
Schlesinger, M.E. and Mitchell, J.F.B., 1987. Climate model simulations of the equilibrium climatic response to increased carbon dioxide. Rev. Geophys., 25: 760–798.
Somerville, R.C.J. and Remer, L.A., 1984. Cloud optical thickness feedbacks in the CO_2 climate problem. J. Geophys. Res., 89: 9668–9672.

Somerville, R.CJ. and Iacobellis, S., 1987. Cloud-radiation interactions: Effects of cirrus optical thickness feedbacks. In: T. Matsuno (Editor), Short- and Medium-Range Numerical Weather Prediction. J. Meteorol. Soc. Jpn., pp. 177–185.
Stephens, G.L., Tsay, S.C., Stackhouse, P.W., Jr. and Flatau, P.J., 1990. The relevance of the microphysical and radiative properties of cirrus clouds to climate and climate feedback. J. Atmos. Sci., 47: 1742–1753.
Takano, Y. and Liou, K.N., 1989. Solar radiative transfer in cirrus clouds. Part I: Single-scattering and optical properties of hexagonal ice crystals. J. Atmos. Sci., 46: 3–19.